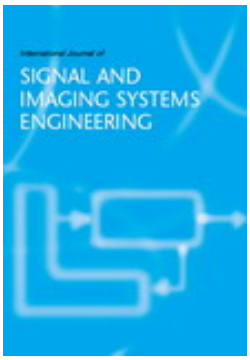

International Journal of Signal and Imaging Systems Engineering

ISSN online: 1748-0701 - ISSN print: 1748-0698
https://www.inderscience.com/ijsise

Segmentation and detection of the retinal vascular network using fast filtering

Nabila Rahmoune, Adel Rahmoune

DOI: 10.1504/IJSISE.2022.10055616

Article History:

Received:	15 October 2020
Last revised:	07 January 2022
Accepted:	10 March 2022
Published online:	28 September 2023

Segmentation and detection of the retinal vascular network using fast filtering

Nabila Rahmoune and Adel Rahmoune*

Faculty of Science,
Department of Computer Science,
Limose Laboratory,
University M'hamed Bougara – Boumerdes,
Boumerdes, 35000, Algeria
Email: n.rahmoune@univ-boumerdes.dz
Email: adel.rahmoune@gmail.com
*Corresponding author

Abstract: Changes in retinal blood vessels are a characteristic sign of many retinal diseases. Therefore, the automatic segmentation of vessels is an essential element for the diagnosis of different ocular diseases. In this paper, we present a novel algorithm for the detection and the segmentation of the vascular network of blood vessels in fundus images. Our algorithm employs two mean linear filters using the convolutional kernel, one directional along a line and the second on a square region, in combination with thresholding. The proposed approach's performance was tested on the public datasets DRIVE and STARE. Based on the test results, the mean segmentation accuracy, sensitivity, specificity and time complexity of retinal images in DRIVE are 94.27%, 97.01%, 66.20% and 1.63 s and for the STARE database, they are 93.41%, 95.54%, 66.55% and 2.13 s respectively. The proposed algorithm is simple and very fast. It achieved satisfactory mean segmentation accuracy with very low time complexity.

Keywords: retinal blood vessel; image segmentation; mean linear filter; retinopathy; directional filtering, thresholding.

Reference to this paper should be made as follows: Rahmoune, N. and Rahmoune, A. (2023) 'Segmentation and detection of the retinal vascular network using fast filtering', *Int. J. Signal and Imaging Systems Engineering*, Vol. 12, No. 4, pp.137–147.

Biographical notes: Nabila Rahmoune holds the degree of Magistere in Computer Science from UQAM, Canada, she is now PhD student and a lecturer at University of Boumerdes, Algeria.

Adel Rahmoune holds PhD in Image Processing from EPFL, Switzerland, he is an Associate Professor at the University of Boumerdes, Algeria.

1 Introduction

In ophthalmology, information about anatomical and pathological structures such as the retinal vascular network of a back-ground image is very important for diagnosis, interpretation, monitoring and therapy of pathologies; such as hypertensive retinopathy (Imran et al., 2019), vascular occlusion and diabetic retinopathy (Wang et al., 2017) due to complications of diabetes mellitus. Diabetic retinopathy is the first factor responsible for reducing the ability to see and is even the major cause of blindness. Early diagnosis and cure can decrease the enduring of cataract patients and prevent visual debilitation from visual impairment (Khawaja et al., 2019; Tavakoli et al., 2017). According to the World Health Organization (WHO), regular screening of diabetics should be performed to study the various physiological and pathological conditions of the retina through retinal image analysis. The only way to detect retinal diseases is through retinal vessel segmentation but it requires retinal experts for manual vessel detection and segmentation (Braovic et al., 2019). However, the number of retinal images to be analysed is too large hence the need to automate the analysis process (Soomro et al., 2019).

In this paper, we present an algorithm for the automated detection of the retinal vascular network which employs medium type linear filters using the convolutional kernel. Several intensity and morphological properties of vascular structures, such as linearity, connectivity and tortuosity's property are considered in our approach. The proposed algorithm is simple, fast and uses few operations in linear time complexity. The method was evaluated using the images of two publicly available databases, the DRIVE (digital retinal images for vessel extraction) and the STARE (structured analysis of the retina) database (Budai et al., 2013). The results of this work are compared with human

observer and those from other recent methods. It shows encouraging performances. The proposed method can serve as one of the first steps in automatic systems whose goal is to detect various retinal abnormalities from retinal fundus images accurately and timely.

This paper is structured as follows. In Section 2, we give an overview of the related work. In Section 3, we present the vascular network segmentation method, i.e., description of the proposed vessel segmentation algorithm. In section 4, we present an evaluation of the proposed method and compare it to various state-of-the-art methods on two publicly available datasets. In Section 5, we give a conclusion and discuss future work.

2 State-of-the-art

The trend towards retinal image analysis has become a competing research focus in recent years. Several factors are conducive,

i the retina is the only place where blood vessels can be visualised non-invasively

ii retinal images can be produced and distributed in a short time and cost

iii retinal vessels are good indicators of many diseases.

Segmentation of the vascular network of the retina is an important step in the process of screening and early detection of certain diseases such as diabetic retinopathy. This allows the detection of anomalies present in the retinal vessels, and therefore the need to have an accurate and a fast algorithm. A large number of supervised and unsupervised methods for the automatic detection of retinal blood vessels from retinal fundus images have been proposed in the literature. We can classify them into five main categories:

i methods based on filtering

ii methods based on mathematical morphology

iii methods based on tracking

iv methods based on classification and learning

v nature-inspired optimisation methods.

Some significant contributions in the field of ophthalmology are given in this section.

2.1 Methods based on filtering

Matched filter (MF) implementation for blood vessel detection is one of the methods giving the most accurate results and is commonly used today in retinal blood vessel detection, (Yin et al., 2015). The matched filter response (MFR) approach was introduced by Chaudhuri et al. (1989). The authors proposed a kernel-based matched filtering mechanism for blood vessel segmentation. It uses 12 different templates that were generated by rotating the actual template by 15 degrees. Hart et al. (1999) proposed the use of curvature to define several measures of tortuosity using skeletonised retinal vessel segments extracted from RGB retinal images. Hoover et al. (2000) proposed a piecewise threshold probing of the MFR for segmenting the blood vessels in retinal images. In Zhang et al. (2016), new unsupervised approach that improves vessel retreading using the adaptive local derived filter (LAD) is presented. Exponential curves are used to adapt to different structures. Yang et al. (2020) proposed Frangi based multi-scale level sets to segment retinal vessels from fundus images. Vascular structures are enhanced by the Frangi filter with local optimal scales being obtained at the same time, then the enhanced image and local optimal scales are considered as inputs of the proposed level set models. Singh and Srivastava (2019) presented a new matched filtering method, which focuses on the equalisation of adaptive histograms with contrast limitation and the matched filter is based on the second Gaussian derivative. Then, an optimal threshold technique based on entropy is used. A new hybrid approach (MF-PSO) is introduced, based on the particle swarm optimisation (PSO) algorithm and the MF technique, which attempts to improve the filter performances (Subudhi et al., 2016). A novel extension of the matched filter (MF) approach, namely the MF-FDOG, is proposed to detect retinal blood vessels. It is composed of the original MF, which is a zero-mean Gaussian function, and the first-order derivative of Gaussian (FDOG). The vessels are detected by thresholding the retinal image's response to the MF, while the threshold is adjusted by the image's response to the FDOG (Zhang et al., 2010).

2.2 Methods based on mathematical morphology

Zana and Klein (1997) proposed the use of mathematical morphology operators to detect retinal vessels, since the vascular network can be considered as a related set of segments. For example, the opening and closing operations, the top-hat operators were used constructively to extract the vessels. Zana and Klein (2001) presented a new algorithm based on mathematical morphology and curvature assessment for the detection of vessel models in a noisy environment, with Gaussian profile. Roychowdhury et al. (2015) described an approach of 3 steps. The pre-processing by a high-pass filter is followed by the extraction of a binary image and then the reconstruction of another binary image from a morphologically improved image. A combination of a Gaussian model classifier (GMM) was applied to classify all remaining pixels from the previous step. In Soumyadeep et al. (2019), an adaptive equalisation technique is introduced, as a pre-treatment, for limited contrast histogram. The morphological grey levels have undergone transformations using multi-structuring element with variable orientations in order to succeed in separating blood vessels from the background. As a last step, a guided thresholding by some morphological operations is used to obtain the image. Dash and Bhoi (2019) proposed a morphological approach to extract blood vessels. They opted for image enhancement and smoothing using CLAHE. Kirsch's technique is adopted to extract blood

vessels and morphological operations to refine the results. Sundaram et al. (2019) proposed a hybrid approach based on morphology and thresholding. Their technique uses morphology, multi-scale vessel enhancement and image fusion for blood vessels. Braovic et al. (2019) presented the optical fundal images segmentation approach.

2.3 Methods based on tracking

Blood vessel tracking methods need a seed point to trace the vasculature. The success of the method depends on the seed point. It consists in defining an initial seed pixel on the centre-line or the edges of retinal vessel, then, from this point, it iteratively tracks retinal vessels according to their characteristics (Moccia et al., 2018). In the tracking-based approach proposed by Chutatape et al. (1998), the retinal blood vessels are detected using a tracking approach with Kalman and Gaussian filters. The average vessel centreline is approximated with a second-order Gaussian filter and the vessel tracking is introduced around the optic disc perimeter. The Kalman filter is used to approximate the location of the next vessel segment. Then, the detection of the vessel branches is tracked. Nayebifar and Moghaddam (2013) presented a new approach based on particle filtering to determine the vessel paths in retina for automatic blood vessel segmentation. Yavuz et al. (2017) described an algorithm that, from a vessel starting point that is generally determined by locating the centre of the DO, the tracking is performed iteratively by selecting the pixels belonging to the retinal vascular tree, through two or three-dimensional adaptive filters. Wang et al. (2018) developed a new algorithm for enhancing and segmenting retinal vessel using multi-scale morphology and seed point tracking approach. At each scale, the high contrast blood vessel images are detected using top-hat and bottom-hat transformation with a line structuring elements which allows for filtering the areas with diameters greater than the scale of the structuring element. The blood vessel image is segmented by multi-threshold based vessel tracking technique. Ciecholewski and Kassjański (2021) distinguish methods that track vessels according to the vascularisation model, and those that determine the minimum cost path between two starting points based on the image-derived metrics.

2.4 Methods based on classification and learning

The classification method is targeted at dividing image pixels into the blood vessel and non-vessel types. It uses various supervised classification techniques considering the feature structure of image vessel to achieve blood vessel segmentation (Abdulsahib et al., 2021). Supervised approaches use ground truth data for the classification of vessels that consider features of the blood vessels. These approaches comprise principal component analysis (Sinthanayothin et al., 1999). Niemeijer et al. (2004) presented a vessel segmentation algorithm based on pixel classification using a simple feature vector. For each pixel, features are extracted from the green-channel image, and a K-nearest neighbourhood (kNN) classifier outputs a soft classification that indicates the probability of being a vessel point. Deep learning technology has developed very rapidly in medical image segmentation; its application mainly covers convolutional neural network (CNN), U-net neural network and recurrent neural network (RNN) (Luo and Jia, 2020). New architectures are proposed, where a multi-level network overseen to retinal vessel segmentation was introduced. This method combined multiple-level lateral output layers to obtain a vessel probability map (Mo and Zhang, 2017; Fu et al., 2016). In Wang et al. (2020) the authors proposed a new deep neural network architecture for retinal blood vessel segmentation, namely, hard attention net (HAnet). It is composed of three decoder networks. The first one dynamically locates which image regions are ‘hard’ or ‘easy’ to analyse and the two other are designed for hard and easy region segmentation. Shin et al. (2019) developed a new deep learning method for vessel segmentation. A convolutional graphic network is integrated into a unified CNN architecture and a combination of unusual characteristic models were applied which allows the final segmentation to be deduced. Son et al. (2019) proposed a generative adversarial network (GAN) approach to segment retinal vessel images and optical disks.

2.5 Methods based on optimisation

Metaheuristics have been extensively used in recent years for retinal vessel segmentation. Cinsdikici et al. (2009) proposed an algorithm that uses matched filtering with ant colony optimisation. Emary et al. (2016) presented multi-objective retinal blood vessels localisation approach based on flower pollination search algorithm (FPSA) and pattern search (PS) algorithm. In Keerthana et al. (2017) firefly algorithm (FA), in combination with a multi-scale matched filter is presented to extract the retinal vessel from retinal image. The proposed algorithm determines the optimal filter parameters of the multi-scale matched filter. Khomri et al. (2018) proposed a multi-objective optimisation method based on the bacterial foraging optimisation algorithm (BFOA) and the artificial bee colony algorithm (ABC). In (Çetinkaya and Duran, 2020), clustering based heuristic ABC, particle swarm optimisation (PSO), differential evolution (DE), teaching learning based optimisation (TLBO), grey wolf optimisation (GWO), firefly (FA) and Harmony Search (HS) algorithms were applied for accurate segmentation of retinal vessels. Devarajan and al, (2020) proposed hybrid approach (HONC), combining unsupervised learning algorithm of three-layer neural networks (NN) and ant colony optimisation algorithm (ACO) as a nature-inspired optimisation algorithm. The method consists of two steps. In the first step, the ACO algorithm is used in order to provide a vector of optimal or appropriate features for using in the classification and learning algorithm. In the second step, the features vector is subjected to intense learning in order to classify pixels in regions that contain or not blood vessels.

3 Proposed vessel segmentation method

In this paper, a new methodology for blood vessel detection is presented. It is based on directional and mean filters with a convolution technique which is the effective way to extract blood vessels. The kernels used are rotated into 12 different orientations on each point of the image to fit into vessels of different directions. The image is then thresholded to extract the vessel skeleton from the background.

3.1 Vascular network segmentation method description

In the Proposed approach, the extraction of the vascular network consists in defining the features, which are determined by means of a filtering operation of medium type in order to include the notion of the neighbourhood and also to delimit the contours of the vessels.

We can see in a retinal image that the blood vessels have a very low level of grey in relation to their neighbourhood, which consists mainly of tissue with a certain texture. In other words, the vessels in the retina are the local minima and also have a very special shape which is that of a «ridge» or a crest, which has a certain height and a certain width. It should be noted that the lesions, which are sometimes present in the retina image, have a grey level which is low, however, these regions can be removed after the detection phase by an appropriate post-treatment procedure. Now, if we take a linear filter of size (n) and in a direction (d) at a given point, which belongs to a vessel, and we calculate the average of this filter in all possible directions, it can be confirmed, experimentally, that this average is minimal in a particular direction, which is that of the direction of the vessel. That is, when the filter support is inside the vessel and aligned with the vessel, as shown in Figure 1(a). In other words, if we take a cross section of a vessel (see Figure 1(b), we designate by x a point outside of the vessel and y another point of the interior of the vessel. When the filter support is aligned with y, the filter response at point x is greater than that of point y, which is minimum of all responses. The point where the local minimum is located is one point inside the vessel. In this technique, blood vessel segmentation uses a linear filter of a segment and a two-dimensional square region mean filters through the convolutional kernel. Twelve directional filters were oriented according to different values of the 12 rotations angles θ. The pre-processed image is convolved with each of the twelve kernels, each rotated into a different orientation. The final response map was computed by taking the minimum response of the 12 kernels at each location. The corresponding mask size is mask_size × mask_size pixels where $masksize = 10$. It is noteworthy that theses kernels were rotated into the angular direction $\theta = 0,15,30, \ldots, 180$ degrees, with the angular step of 15 degrees in order to cover all possible directions of blood vessel segments. A joint image is then obtained by the selection of the minimum response as shown in Figure 1. Then, the ratio of the mean filter to directional filter response (see Figure 2) was calculated. For this step, we apply also the square mean filter of the same size as the directional mean filter, e.g., 10 by 10 to the image. Next, we take the ratio between the output of the directional filter and the square mean filter. After that, we threshold this ratio in order to obtain a binary representation of the vascular tree.

Figure 1 An illustration of directional filters on a vessel segment: (a) the filter response is minimal when the filter support is inside the vessel and aligned with it and (b) slice of a vessel where x is a point of the vessel and y is a point that is inside and aligned with the filter support

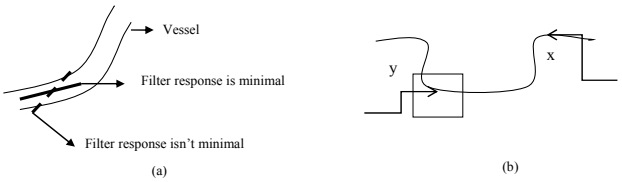

Figure 2 Localisation of the vessel's direction

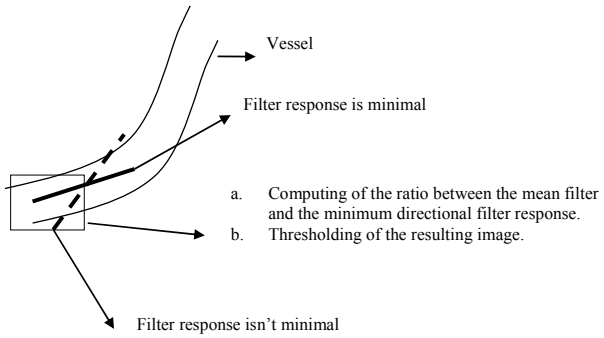

3.2 Proposed algorithm

Retinal image is segmented through the following steps:

1 Extract the green channel of the image to be processed. Let imageG be the green channel image.

2 For each angle (direction) θ, $\theta = 0,15,30, 45,\ldots,180$ degrees, with the angular step of 15 degrees, construct masks k_i with size mask_size, for the i direction, $i = 1..12$, where the new coordinate are calculated by equation (1).

$$\begin{cases} x(m) = (m - mask\_size/2) * \sin(theta) \\ y(m) = (m - mask\_size/2) * \cos(theta) \\ m = 1..mask\_size \end{cases} \quad (1)$$

2.1 Filter k_i is then filled with 1's as in equation (2)

$$mask(u\,\text{int}\,8(x(m)) + 0.5 + mask\_size/2), u\,\text{int}\,8(y(m) \\ 0.5 + \text{mask\_size}/2)) = 1 \quad (2)$$

3 The average value of each point of the Kernel k_i is calculated by equation (3)

$$mask(i,j) = \frac{mask(i,j)}{\sum_{il=1}^{mask\_size}\sum_{ic}^{mask\_size} mask(il,ic)} \quad (3)$$

3.1 Apply the K_i filter to each point of the 12 images. Let imageG_filtered, be the resulted image;

3.2 For each point of imageG_filtered, select the one having the minimum response from the 12 direction, this filter points to the direction of the blood vessel. Let imageG_min be the result image;

3.3 Apply also the square mean filter of the same size, e.g., 10 by 10 to imageG and obtain imageG_filtered_square as result.

4 Take the ratio between imageG_filtered_square and imageG_min then threshold it to produce the image of blood vessels.

3.3 Implementation of the algorithm

We implemented the method using MATLAB 2015 (R2015a) programming software, for its efficiency to be able to test the concepts quickly. Evaluation of the algorithm was performed on a personal computer with Intel® Core™ i5 processor, 4 GB system memory, and Windows®10 Professional 64-bit operating system. As a first step, the green channel of the image is extracted for processing since it contains maximum contrast between blood vessels and other retinal structures as shown in Figure 3. Also, Green channel image produces better results. Then, a further improvement, by a non-linear transformation of intensity, is made on the extracted image. It is made by the matlab imadjust tool which allows to transform the levels of the image {min, max} in the range {0,255}. Therefore the brightness will be uniform for all points and the result will not depend on the brightness.

Figure 3 Illustration of pre-processing: (a) the original colour retinal fundus image; (b) the red channel of the image; (c) the green channel of the image and (d) the blue channel of the image (see online version for colours)

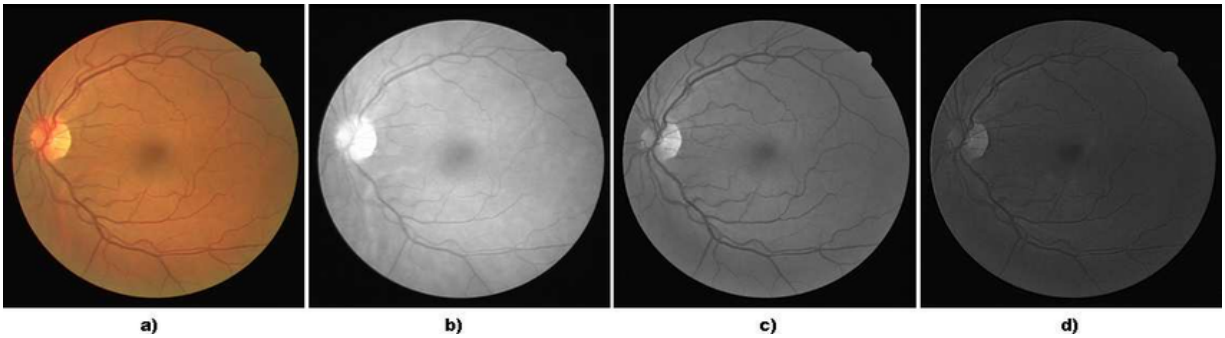

Figure 4 Image from DRIVE database: (a) original test image; (b) grey-scaled image and (c) ground truth image (see online version for colours)

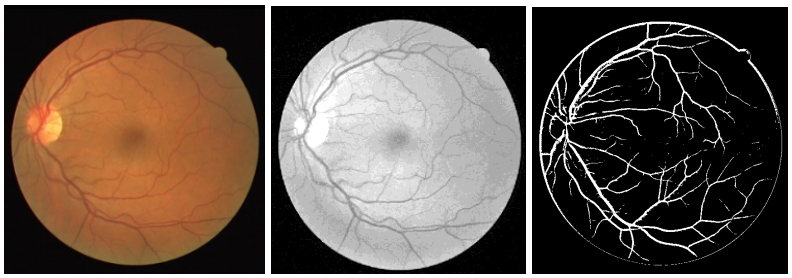

4 Experimental results and discussion

4.1 Datasets and performance measures

In order to evaluate the performances of the proposed algorithm for the blood vessel segmentation in the retinal fundus images and to compare it with the different methods present in the state-of-the-art, we have used two public benchmark datasets, the DRIVE and the STARE databases which are the most commonly used. The images of the DRIVE database were acquired from Canon CR5 non-mydriatic 3CCD camera with a 45° field of view (FOV). The captured images contain 8 bits per colour plane at 768×584 pixels. The ground truth image was manually segmented and segmentation process was performed by the observers. These 40 images were divided into two sets: a test set and a training set. Each set contains 20 original retinal images together with respective ground truth images as shown in Figure 4. The STARE database contains 20 retinal images and out of 20 images there are 10 healthy retinal fundus images and the remaining belongs to unhealthy retinal images. These images were captured by a TopCon TRV-50 fundus camera at 35° field of view. The captured images contain 8 bits per colour channel at 650×500 pixels. The ground truth image was manually segmented and segmentation process was performed by two observers.

The performance comparison of the proposed algorithm is realised based on the sensitivity (Se), specificity (Sp), accuracy (Acc) and execution time (second). These measures have been computed individually for each image and on average for the whole test images. These metrics are defined as follows:

$$Se = \frac{\mathrm{TP}}{\mathrm{TP} + \mathrm{FN}} \tag{4}$$

$$Sp = \frac{\mathrm{TN}}{\mathrm{TN} + \mathrm{FP}} \tag{5}$$

$$Acc = \frac{\mathrm{TP} + \mathrm{TN}}{\mathrm{TP} + \mathrm{FN} + \mathrm{TN} + \mathrm{FP}} \tag{6}$$

True positive (TP) corresponds to the vessel pixels properly detected as vessel pixels, false negative (FN) represents the number of vessel pixels wrongly detected and true negative (TN) is the number of non-vessel pixels properly detected as non-vessel pixels. The sensitivity and specificity parameters measure the approach's ability to properly detect blood vessel pixels and background ones, respectively. The Accuracy (Acc) can be the proportion of true positive and true negative in all evaluated cases. It is an approximation of measurement results to the true value, according to gold standard hand labelled segmentation.

4.2 *Parameter fitting*

In our approach, we have two key parameters to determine and set; the optimal threshold Th and the mask size n × n for mean linear filtering. These parameters were chosen based on our experiments simulations. The experimental values of thresholds are Th = 1.05 and 1.04 for the DRIVE (manual and training images) and STARE databases respectively provided the best compromise value between average accuracy and sensitivity in each database.

For the same given threshold value, accuracy and sensitivity are calculated for all images in the same database. Then, the average of these values is calculated. This process is repeated for the different values of the threshold from 0.80 to 1.09 step of 0.01. At the value of threshold Th = 1.05 and 1.04 for all images of the DRIVE and STARE databases respectively, the accuracy averages are maximum respectively 0.9425 and 0.9341 with sensitivity 0.9701 and 0.9554 respectively. Beyond these threshold values, the accuracy average decreases as shown in Figure 5.

The mask size n×n was set to 10×10 in an experimental way also. The proposed method was executed with different values of n, starting with $n = 8$ to 26 in steps of 2. The best segmentation for all images from the DRIVE and STARE databases was obtained for $n = 10$ as shown in Figure 6, where the accuracy and sensitivity average compromise are maximum.

Figure 5 The average Acc value as a function of the threshold parameter for the DRIVE and STARE datasets (see online version for colours)

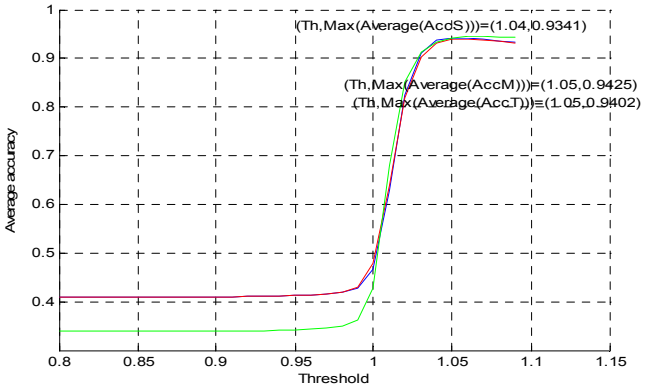

Figure 6 The average Acc value as a function of the mask size parameter for the DRIVE and STARE datasets (see online version for colours)

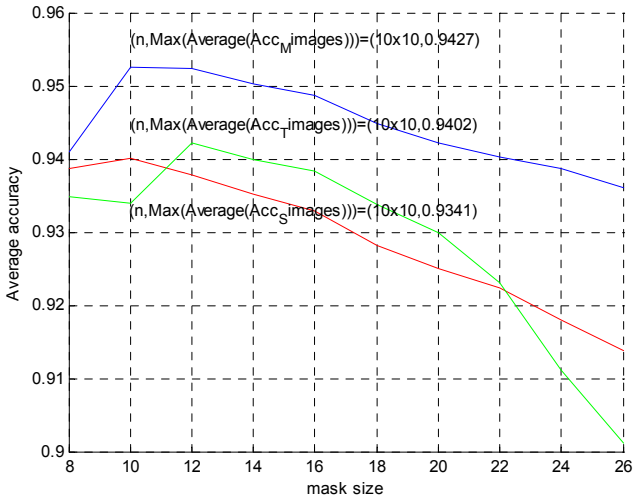

4.3 *Analysis and comparison*

The primary motivation behind this research work is developing a fast and simple algorithm, automated for retinal blood vessel segmentation. The set of images are applied to the algorithm and the measures computed using equations (4)–(6) are presented in Tables 1–3.

The average values of these tables confirm that the proposed method offers satisfactory result on the DRIVE and STARE databases chosen for the study. Figure 7 presents the segmentation result for images DRIVE and STARE datasets. The outcome of the proposed approach is then validated using a comparative study between the extracted vessel and the gold standard segmentations existing in the database. Figure 8 presents the pixelwise comparison of the chosen ground truth image and extracted vessel image. All results are obtained by using the same threshold value: 1.05 and 1.04 for DRIVE and STARE

images datasets respectively with mask_size = 10*10. The mean segmentation accuracy, sensitivity, specificity and time complexity of retinal images in DRIVE are 94.27%, 97.01%, 66.20% and 1.63s and for the STARE are 93.41%, 95.54%, 66.55% and 2.13s respectively.

Table 1 Performance results on manual DRIVE dataset images

Image	*Se*	*Sp*	*Acc*	*Time*(s)
1	0.6899	0.9749	0.9494	1.62
2	0.6909	0.9762	0.9470	1.63
3	0.6860	0.9638	0.9361	1.63
4	0.6913	0.9705	0.9448	1.63
5	0.6453	0.9761	0.9452	1.63
6	0.5632	0.9793	0.9388	1.63
7	0.6540	0.9722	0.9431	1.64
8	0.5755	0.9712	0.9372	1.63
9	0.4392	0.9835	0.9394	1.63
10	0.6787	0.9716	0.9475	1.64
11	0.6869	0.9704	0.9450	1.64
12	0.6498	0.9751	0.9470	1.63
13	0.5402	0.9796	0.9366	1.63
14	0.7061	0.9681	0.9470	1.64
15	0.8522	0.9055	0.9017	1.64
16	0.6252	0.9791	0.9471	1.63
17	0.4918	0.9802	0.9390	1.64
18	0.6363	0.9784	0.9513	1.64
19	0.8391	0.9627	0.9524	1.63
20	0.6772	0.9764	*0.9561*	1.64
Average	*0.6620*	*0.9701*	*0.9427*	*1.63*

Table 2 Performance results on training DRIVE dataset images

Image	*Se*	*Sp*	*Acc*	*Time* (s)
1	0.6132	0.9793	0.9519	1.61
2	0.6325	0.9755	0.9445	1.61
3	0.6767	0.9601	0.9414	1.63
4	0.5574	0.9792	0.9304	1.63
5	0.4515	0.9804	0.9296	1.62
6	0.7325	0.9550	0.9364	1.63
7	0.6140	0.9754	0.9435	1.63
8	0.6011	0.9784	0.9416	1.62
9	0.7339	0.9610	0.9419	1.62
10	0.7155	0.9589	0.9398	1.62
11	0.6728	0.9695	0.9516	1.63
12	0.5646	0.9807	0.9467	1.63
13	0.5939	0.9798	0.9486	1.62
14	0.7206	0.8947	0.8776	1.61
15	0.7719	0.9663	0.9495	1.63
16	0.6658	0.9750	0.9414	1.63

Table 2 Performance results on training DRIVE dataset images (continued)

Image	*Se*	*Sp*	*Acc*	*Time* (s)
17	0.7498	0.9643	0.9456	1.63
18	0.5209	0.9810	0.9413	1.63
19	0.6729	0.9734	0.9476	1.62
20	0.7957	0.9671	0.9541	1.63
Average	*0.6529*	*0.9677*	*0.9402*	*1.62*

Table 3 Performance results on STARE dataset images

Image	*Se*	*Sp*	*Acc*	*Time* (s)
1	0.7033	0.9546	0.9346	2.14
2	0.5665	0.9497	0.9241	2.14
3	0.8133	0.9435	0.9357	2.13
4	0.2318	0.9869	0.9309	2.14
5	0.7577	0.9368	0.9206	2.13
6	0.8515	0.9391	0.933	2.13
7	0.7718	0.9374	0.9242	2.13
8	0.6453	0.9302	0.9089	2.12
9	0.8803	0.9565	0.9505	2.14
10	0.7045	0.9292	0.9111	2.14
11	0.9073	0.9394	0.9371	2.16
12	0.8992	0.9533	0.9491	2.17
13	0.8093	0.9568	0.9436	2.14
14	0.7953	0.9603	0.9453	2.14
15	0.6133	0.9769	0.9455	2.14
16	0.5056	0.9764	0.9283	2.15
17	0.6544	0.9326	0.9077	2.15
18	0.518	0.9818	*0.9584*	2.13
19	0.4315	0.9848	0.961	2.13
20	0.2512	0.9823	0.9335	2.12
Average	*0.6655*	*0.9554*	*0.9341*	*2.13*

Finally, a detailed assessment is performed by considering the average values of the sensitivity, specificity, accuracy and execution time of the proposed approach with the results of other methods existing in the literature as shown in Tables 4 and 5.

Table 4 Performance measures for DRIVE and STARE datasets

Dataset	*Method*	*Se*	*Sp*	*Acc*	*Time* (s)
DRIVE (Manual, Training)	*Proposed method*	*0.6620*	*0.9701*	*0.9427*	*1.63*
		0.6529	*0.9677*	*0.9402*	*1.62*
	2nd human observer	0.7760	0.9724	0.9472	–
STARE	*Proposed method*	*0.6655*	*0.9554*	*0.9341*	*2.13*
	2nd human observer	0.8952	0.9384	0.9349	–

Figure 7 The segmentation result for images DRIVE (first row) and STARE (second row) datasets: (a) original test image;(b) grey-scaled image;(c) ground truth image and (d) thresholded image with proposed method (see online version for colours)

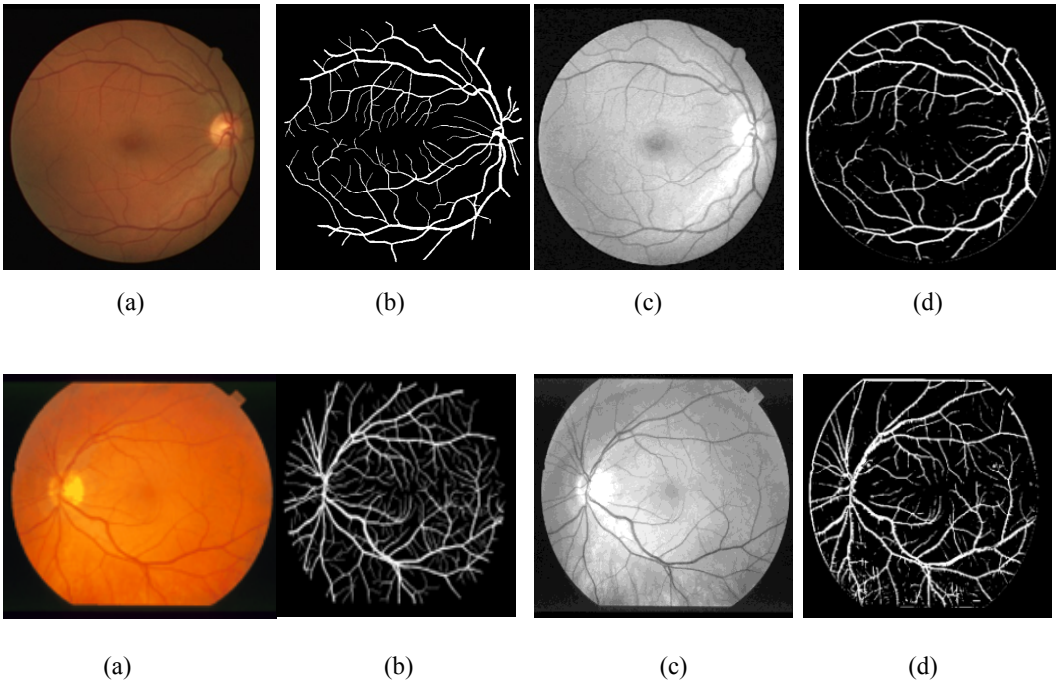

Figure 8 Comparison of the best (a) and the worst (b) segmentation results measured by A_{cc} using DRIVE and STARE datasets respectively. The first and second lines: original test image and gold standard segmentations respectively, the third one results of the proposed method (see online version for colours)

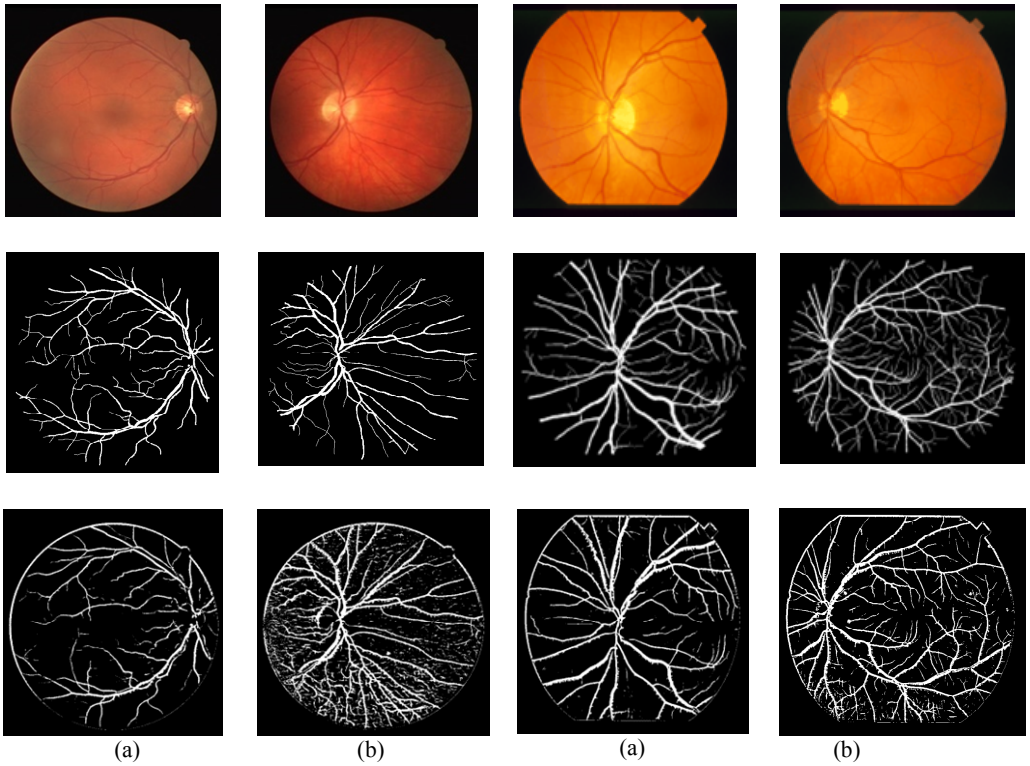

Table 5 Comparison of the performance of the proposed approach with other methods on DRIVE and STARE datasets in terms of execution time, accuracy, sensitivity and specificity

Test data	*DRIVE*				*STARE*			
Vessel detection method	*Se*	*Sp*	*Acc*	*Time(s)*	*Se*	*Sp*	*Acc*	*Time(s)*
Supervised								
Budai et al. (2013)	0.644	0.987	0.957	5	0.580	0.982	0.938	6
Li et al. (2016)	0.981	0.952	0.973	62	0.772	0.984	0.962	62
Liskowski and Krawiec (2016)	0.781	0.980	0.953	92	0.855	0.986	0.972	92
Fu et al. (2016)	0.729	–	0.947	21.5	0.714	–	0.954	–
Mo et al. (2017)	0.814	0.984	0.952	0.4	0.766	0.981	0.959	–
Unsupervised								
Zhang et al. (2010)	0.712	0.972	0. 938	–	0.717	0.975	0.948	10
Fraz et al. (2012)	0.715	0.975	0.943	120	0.731	0.968	0.944	120
Nguyen et al. (2013)	0.698	0.972	0.941	5.6	0.836	0.945	0.932	–
Hassanien et al. (2015)	0.721	0.971	0.938	–	0.649	0.982	0.946	–
Emary et al. (2016)	–	–	0.936	102	–	–	–	–
Subudhi et al. (2016)	0.345	0.970	0.911	–	–	–	–	–
Zhang et al. (2016)	0.774	0.972	0.947	20	–	–-	–-	–
Yavuz and Köse (2017	–	0.970	0.959	8.6	–	0.981	0.943	9.13
Keerthana et al. (2017)	0.791	0.980	0.871	–	–	–	–	–
Khomri et al. (2018)	0.739	0.974	0.945	2.21	0.737	0.962	0.940	3.14
Wang et al. (2018)	0.723	0.981	0.944	–	0.748	0.968	0.946	–
Braovic et al. (2019)	0.702	0.988	0.963	–	0.695	0.982	0.961	–
Dash et al. (2019)	0.774	0.974	0.951	–	–	–	–	–
Khawaja et al. (2019)	0.804	0.973	0.955	5	0.801	0.969	0.954	5
Shin et al. (2019)	0.927	0.925	0.938	–	0.937	0.935	0.959	–
Singh et al. (2019)	0.773	0.046	0.937	–	0.838	0.092	0.893	–
Soumyadeep et al. (2019)	0.612	0.974	0.943	–	–	–	–	–
Sundaram et al. (2019)	0.691	0.941	0.931	–	–	–	–	–
Çetinkaya et al. (2020)	0.831	0.980	0.965	–	0.837	0.978	0.960	–
Devarajan et al. (2020)	0.801	0.789	0.979	13.01	0.864	0.801	0.979	15.94
Wang et al. (2020)	0.799	0.981	0.958	–	–	–	–	–
Yang et al. (2020)	0.734	0.974	0.953	2.3	0.773	0.957	0.943	–
Proposed method	*0.662*	*0.970*	*0.942*	*1.62*	*0.665*	*0.955*	*0.934*	*2.13*

The proposed approach is very fast, because it uses fewer operations. The temporal complexity is calculated. It's dominated by the evaluation of step 3.2 of the algorithm. It is θ (L×C), where L×C is the size of the image, it runs in linear time

From these results, it can be noted that, the proposed approach offers an improved execution time more than the alternatives considered in this study. The accuracy is also better and very close to the methods recently discussed by Sundaram et al.(2019), Soumyadeep et al. (2019), Singh et al. (2019), Shin et al. (2019), Keerthana et al. (2017), Subudhi et al. (2016), Emary et al. (2016) and Fu et al. (2016). But it is lower than the methods presented by Braovic et al. (2019) and Çetinkaya and Duran (2020) and it can be improved using hybridisation approach.

The proposed algorithm has advantages that it is very simple, easy to implement and fast in linear time complexity.

5 Conclusion

In the present paper a new algorithm in linear time complexity based on two mean linear filters using the convolutional kernel is implemented to segment the blood vessels from retinal image dataset. It was evaluated on the publicly available DRIVE and STARE datasets on which it achieved the average accuracy of 94.27% and 93.41%, with run time 1.63 s and 2.13 s respectively. A comparative study between the proposed method and other methods in the

literature confirms that the proposed algorithm is efficient in offering low time complexity and satisfactory values of the accuracy.

This novel algorithm differs from others by its simplicity and speed. It employs a few operations which facilitates the implementation and parameters adjusting.

In future work, we intend to expand the research proposed in this paper by hybridising it with other methods proposed recently.

References

Abdulsahib, A.A., Mahmoud, M.A., Mohammed, M.A., Rasheed, H.H., Mostafa, S.A. and Maashi, M.S. (2021) 'Comprehensive review of retinal blood vessel segmentation and classification techniques: intelligent solutions for green computing in medical images, current challenges, open issues, and knowledge gaps in fundus medical images', *Netw. Model. Anal. Health Inform. Bioinform.*, Vol. 10, pp.1–32.

Braovic, M., Stipanicev, D. and Šeric, L. (2019) 'Retinal blood vessel segmentation based on heuristic image analysis', *Comput Sci Inf Syst*, Vol. 16, No. 1, pp.227–245.

Budai, A., Bock, R., Maier, A., Hornegger, J. and Michelson, G. (2013) 'Robust vessel segmentation in fundus images', *International Journal of Biomedical Imaging*, Vol. 2013.

Çetinkaya, M.B. and Duran, H.A. (2020) 'detailed and comparative work for retinal vessel segmentation based on the most effective heuristic approaches', *Biomed Tech* (*Berl*)., Vol. 66, No. 2, pp.181–200.

Chaudhuri, S., Chatterjee, S., Katz, N., Nelson, M. and Goldbaum, M. (1989) 'Detection of blood vessels in retinal images using two-dimensional matched filters', *IEEE Trans Medi Imaging,* pp.263–269.

Chutatape, O., Zheng, L. and Krishnan, S. (1998) 'Retinal blood vessel detection and tracking by matched gaussian and kalman filters', *in: Engineering in Medicine and Biology Society. Proceedings of the 20th Annual International Conference of the IEEE*, Vol. 6, pp.3144–3149.

Ciecholewski, M. and Kassjański, M. (2021) 'Computational methods for liver vessel segmentation in medical imaging', *A Review. Sensors*, Vol. 21, No. 6, p.2027.

Cinsdikici, M.G. and Aydın, D. (2009) 'Detection of blood vessels in ophthalmoscope images using MF/ant', *Computer Methods and Programs in Biomedicine*, Vol. 96, No. 2, pp.85–95.

Dash, J. and Bhoi, N. (2019) 'Retinal blood vessel extract-tion using morphological operators and kirsch's template', *Soft Computing and Signal Processing*, Springer, Singapore, pp.603–611.

Devarajan, D., Ramesh, S.M. and Gomathy, B. (2020) 'A metaheuristic segmentation framework for detection of retinal disorders from fundus images using a hybrid ant colony optimization', *Soft Computing*, Vol. 24, No. 17, pp.13347–13356.

Emary, E., Zawbaa, H.M., Hassanien, A.E. and Parv, B. (2016) 'Multi-objective retinal vessel localization using flower pollination search algorithm with pattern search', *Advances in Data Analysis and Classification*, Vol. 11, No. 3, pp.611–627.

Fraz, M.M., Remagnino, P., Hoppe, A., Uyyanonvara, B., Rudnicka, A.R., Owen, C.G. and Barman, S.A. (2012) 'Blood vessel segmentation methodologies in retinal images–a survey', *Computer Methods and Programs in Biomedicine*, Vol. 108, No. 1, pp.407-433.

Fu, H., Xu, Y., Wong, Dwk. and Liu, J. (2016) 'Retinal vessel segmentation via deep learning network and fully-connected conditional random fields', *13th Int. Symp. Biomed. Imaging (ISBI)*, IEEE, Prague, Czech Republic, pp.698–701.

Hart, W., Goldbaum, M., Cote, B., Kube, P. and Nelson, M. (1999) 'Measurement and classification of retinal vascular tortuosity', *Int. J. Med. Inf.*, Vol. 53, pp.239–252.

Hassanien, A.E., Emary, E. and Zawbaa, H.M (2015) 'Detection blood vessel localization approach based on bee colonyswarm optimization, fuzzy c-means and pattern search', *Journal of Visual Communication and Image Representation*, Vol. 31, pp.186–196.

Hoover, A., Kouznetsova, V. and Goldbaum, M. (2000) 'Locating blood vessels in retinal images by piecewise threshold probing of matched filter response', *IEEE Trans Med Imaging,* pp.203–210.

Imran, A., Li, J., Pei, Y., Yang, J-J. and Wang, Q. (2019) 'Comparative analysis of vessel segmentation techniques in retinal images', *IEEE Access*, Vol., No. 7, pp.114862–114887.

Keerthana, K., Jayasuriya, T.J., Sri Madhava Raja, N. and Rajinikanth, V. (2017) 'Retinal vessel extraction based on firefly algorithm guided multi-scale matched filter', *International Journal of Modern Science and Technology*, Vol. 2, No. 2, pp.74–80.

Khawaja, A., Khan, T.M., Khan, M.A.U. and Nawaz, S.J. (2019) 'A multi-scale directional line detector for retinal vessel segmentation', *Sensors* (*Basel*), Vol. 19, No. 22, p.4949.

Khomri, B., Christodoulidis, A., Djerou, L., Babahenini, M. and Cheriet, F. (2018) 'Retinal blood vessel segmentation using the elite-guided multi-objective artificial bee colony algorithm', *IET Image Processing*, Vol. 12, No. 12, pp.2163–2171.

Li, Q. and Fengn, Xie, B.L. (2016) 'Acrossmodality learning approach for vessel segmentation in retinal images', *IEEE Trans. Med. Imag.*, Vol. 35, No. 1, pp.109–118.

Liskowski, P. and Krawiec, K. (2016) 'Segmenting retinal blood vessels with deep neural networks', *IEEE Trans. Med. Imaging*, Vol. 35, No. 11, pp.2369–2380.

Luo, Z.L. and Jia, Y.B. (2020) 'The comparison of retinal vessel segmentation methods in fundus images', *Journal of Physics: Conference Series*, Vol. 1574, p.012160.

Mo, J. and Zhang, L. (2017) 'Multi-level deep supervised networks for retinal vessel segmentation', *Int. J. Comput. Assist. Radiol.* Surg., Vol. 12, No. 12, pp.2181–2193.

Moccia, S., De Momi, E., El Hadji, S. and Mattos, L.S. (2018) 'Blood vessel segmentation algorithms– review of methods, datasets and evaluation metrics', *Comput Methods Programs Biomed.*, Vol. 158, pp.71–91.

Nayebifar, B. and Moghaddam, H.A. (2013) 'A novel method for retinal vessel tracking using particle lters', *Computers in Biology and Medicine*, Vol. 43, No. 5, pp.541–548.

Nguyen, U.T., Bhuiyan, A., Park, L.A. and Ramamohanaro, K. (2013) 'An effective retinal blood vessel segmentation method using multi-scale line detection', *Pattern Recognition*, Vol. 46, No. 3, pp.703–715.

Niemeijer, M., Stall, B., van Ginneken, B., Loog, M. and Abramoff, M. (2004) 'Comparative study of retinal vessel segmentation methods on a new publicly available database', *SPIE Med. Imag.*, pp.648–656.

Roychowdhury, S., Koozekanani, D.D., Parhi, K.K., Bailie, J.R. and Hart, P.M. (2015) 'Blood vessel segmentation of fundus images by major vessel extraction and sub-image classification', *Biomedical and Health Informatics, IEEE Journal*, pp.2168–2194.

Shin, S.Y., Lee, S., Yun, I.D. and K.M. (2019) 'Deep vessel segmentation by learning graphical connectivity', *Medical Image Analysis*, Elsevier.

Singh, N.P. and Srivastava, R. (2019) 'Extraction of retinal blood vessels by using an extended matched filter based on second derivative of gaussian', *Proceedings of the National Academy of Sciences, India Section A: Physical Sciences*, Vol. 89, No. 2, pp.269–277.

Sinthanayothin, C., Boyce, J., Cook, H. and Williamson, T. (1999) 'Automated localization of the optic disc, fovea, and retinal blood vessels from digital color fundus images', *Br J. Ophtalmol*, pp.902–910.

Son, J., Park, S.J. and Jung, K.H. (2019) 'Towards accurate segmentation of retinal vessels and the optic disc in fundoscopic images with generative adversarial networks', *J. Digit Imaging*, Vol. 32, No. 3, pp.499–512.

Soomro, T.A., Afifi, A.J., Ali Shah, A., Soomro, S., Baloch, G.A., Zheng, L., Yin, M. and Gao, J. (2019) 'Impact of image enhancement technique on cnn model for retinal blood vessels segmentation', *IEEE*, Vol. 7, pp.158183–158197.

Soumyadeep, P., Saptarshi, C., Debangshu, D. and Munshi, S. (2019) 'Morphological operations with iterative rotation of structuring elements for segmentation of retinal vessel structures', *Multidim Syst Sign Process*, Vol. 30, pp.373–389.

Subudhi, A., Pattnaik, S. and Sabut, S. (2016) 'Blood vessel extraction of diabetic retinopathy using optimized enhanced images and matched filter', *J. Med. Imag*, Vol. 3, No. 4, pp.044003.

Sundaram, R., Jayaraman, R.K.P. and Venkatraman, B. (2019) 'Extraction of blood vessels in fundus images of retina through hybrid segmentation approach', *Mathematics*, Vol. 7, No. 2, p.169.

Tavakoli, M., Nazar, M., Golestaneh, A. and Kalantari, F. (2017) 'Automated optic nerve head detection based on different retinal vasculature segmentation methods and mathematical morphology', *IEEE Nuclear Science Symposium and Medical Imaging Conference (NSS/MIC)*, Atlanta, USA, p.17.

Wang, D., Haytham, A., Pottenburgh, J., Saeedi, O. and Tao, Y. (2020) 'Hard attention net for automatic retinal vessel segmentation', *IEEE J. Biomed Health Inform*, Vol. 24, No. 12, pp.3384–3396.

Wang, S., Tang, H.L., Al Turk, L.I., Hu, Y., Sanei, S, Saleh, G.M. and Peto, T. (2017) 'Localizing microaneurysms in fundus images through singular spectrum analysis', *IEEE Transactions on Biomedical Engineering*, Vol. 64, No. 5, pp.990–1002.

Wang, W., Zhang, J., Wu, W. and Zhou, S. (2018) 'An automatic approach for retinal vessel segmentation by multi-scale morphology and seedpoint tracking', *Journal of Medical Imaging and Health Informatics*, Vol. 8, No. 2, pp.262–274.

Yang, J., Huang, M., Fu, J., Lou, C. and Feng Frangi, C. (2020) 'Frangi based multi-scale level sets for retinal vascular segmentation', *Comput Methods Programs Biomed*, Vol. 197, p.105752.

Yavuz, Z. and Köse, C. (2017) 'Blood vessel extraction in color retinal fundus images with enhancement filtering and unsupervised classification', *J. Healthc. Eng.*, Vol. 2017.

Yin, B., Li, H., Sheng, B., Hou, X., Chen, Y., Wu, W. and Jia, W. (2015) 'Vessel extraction from non-fluorescein fundus images using orientation-aware detector', *Med. Image Anal.*, Vol. 26, No. 1, pp.232–242.

Zana, F. and Klein, J. (1997) 'Robust segmentation of vesssels from retinal angiography', *International Conference on Digital Signal Processing*, Santorini, Greece, pp.1087–1090.

Zana, F. and Klein, J. (2001) 'Segmentation of vessel-like patterns using mathematical morphology and curvature evaluation', *IEEE Transactions on Image Processing*, Vol. 10, No. 7, pp.1010–1019.

Zhang, B., Zhang, L., Zhang, L. and Karray, F. (2010) 'Retinal vessel extraction by matched filter with first-order derivative of gaussian', *Comput. Bio.*, Vol. 40, No. 4, pp.438–445.

Zhang, J., Dashtbozorg, B., Bekkers, E., Pluim, J.P., Duit, R. and Ter Haar Romeny, B.M. (2016) 'Robust retinal vessel segmentation via locally adaptive derivative frames in orientation scores', *IEEE Trans Med Imaging*, Vol. 35, No. 12, pp.2631–2644.